

Effect of Double Bond Position on Dehydroergosterol Fluorescence Intensity Dips in Phosphatidylcholine Bilayers with Saturated *sn*-1 and Monoenoic *sn*-2 Acyl Chains

Mei Mei Wang,[†] Istvan P. Sugar,[‡] and Parkson Lee-Gau Chong^{*,†}

Department of Biochemistry, Temple University School of Medicine, Philadelphia, Pennsylvania 19140, and Departments of Biomathematical Sciences and Physiology & Biophysics, Mount Sinai Medical Center, New York, New York 10029

Received: March 1, 2002; In Final Form: April 11, 2002

We have investigated the spectroscopic evidence for sterol superlattice formation in bilayers composed of dehydroergosterol (DHE) and a homologous series of phosphatidylcholine, namely, C(18:0):C(18:1 Δ^n)PC with $n = 6, 7, 9, 11$, and 13 . These phosphatidylcholines (PCs) possess the same number of carbons and the same number of cis double bonds; however, the position of the double bond of these PCs varies. We have examined the fractional concentration dependence of the steady-state fluorescence intensity of DHE in the liquid-crystalline multilamellar vesicles composed of DHE and this series of PCs. The DHE contents in the membranes were varied by ~ 0.2 mol % in two concentration regions, 18.7 – 21.3 and 23.9 – 26.0 mol % DHE. In these two regions, 20.0 and 25.0 mol % are the critical sterol mole fractions predicted for maximal superlattice formation. A DHE intensity dip appears at each of these two critical sterol mole fractions in the PC bilayers that have the double bond located between C9 and the terminal carbon. However, no distinct DHE intensity dips are observed in these two concentration regions as well as in the region 18.4 – 27.5 mol % DHE, when the double bond is located at C6–C7 or C7–C8. These data suggest that sterol superlattice can occur in liquid-crystalline state of unsaturated phospholipid bilayers so long as the cis double bonds are not located between C9 and the carboxyl carbon. It appears that appropriate van der Waals contacts between the steroid ring and the C2–C9 segment of the phospholipid acyl chain are required for sterol superlattice formation.

Introduction

Dehydroergosterol ($\Delta^{5,7,9,(11),22}$ -ergostatetraene- 3β -ol, DHE, Figure 1) is a naturally occurring fluorescent sterol found in the Red Sea sponge *Biemna fortis* and resembles both cholesterol and ergosterol in its physical and physiological properties.^{1–4} In a previous study of sterol lateral organization in bilayer membranes, we used DHE as both a fluorescent sterol probe and a membrane component.⁵ It was found that the plot of the DHE fluorescence versus the mole fraction of DHE (X_{DHE}) in liquid crystalline dimyristoyl-L- α -phosphatidylcholine (DMPC) bilayers shows a number of intensity drops, referred to as the dehydroergosterol intensity dips (or DHE dips). The dips appear at or very close to the critical mole fractions theoretically predicted for sterols being regularly distributed into hexagonal superlattices.^{4,5} In this case, the DMPC acyl chains form a hexagonal host lattice in the plane of the membrane and DHE fits into one or two lattice points, but DHE molecules are maximally separated, thus forming a hexagonal superlattice within the hexagonal host lattice.^{4,5} Additional spectroscopic evidence of this sort for sterol superlattice formation was subsequently obtained from other DHE fluorescent parameters^{6,7} and from nonsterol fluorescent probes.^{6,8–11} More recently,

evidence for sterol superlattice formation was also found in functional assays of membrane surface acting enzymes.^{12–14}

Sterol superlattice formation was not confined to saturated phosphatidylcholine (e.g., DMPC) bilayers. It also occurred in liquid crystalline sphingomyelin,⁶ 1-palmitoyl-2-oleoyl-L- α -phosphatidylcholine (POPC) and POPC/1-palmitoyl-2-oleoyl-L- α -phosphatidylethanolamine (POPE) mixed bilayers.¹¹ POPC and POPE each contain one cis double bond in the *sn*-2 acyl chain at the C9–C10 position counting from the carboxyl carbon. The observation of evidence for sterol superlattice formation in POPC and POPC/POPE bilayers¹¹ is of biological interest, because most phospholipids in cell membranes are *sn*-1-saturated and *sn*-2-unsaturated, and POPC is the most abundant phosphatidylcholine (a major phospholipid class) in mammalian liver cell membranes. Moreover, in mammals, the first double bond introduced to saturated fatty acids by *de novo* synthesis almost always occurs at the position between C9 and C10, as in the case of oleic acid in POPC and POPE. However, in biological membranes, the position and the number of the cis double bond in the *sn*-2 acyl chain of membrane phospholipids may vary considerably. Whether these variations would affect the formation of sterol superlattice in the membrane remained unexplored.

In the present study, we have examined the fractional concentration dependence of the steady-state fluorescence intensity of DHE in the liquid-crystalline state of DHE/C(18:0):C(18:1 Δ^n)PC bilayers with $n = 6, 7, 9, 11$, and 13 (structures illustrated in Figure 1). These phosphatidylcholines (PCs) possess the same number of carbons and the same number of cis double bonds; however, the position of the double bond of

* To whom correspondence should be addressed. Department of Biochemistry, Temple University School of Medicine, 3420 N. Broad Street, Philadelphia, PA 19140. Phone: (215) 707-4182. Fax: (215) 707-7536. E-mail: pchong02@unix.temple.edu.

[†] Department of Biochemistry.

[‡] Departments of Biomathematical Sciences and Physiology & Biophysics.

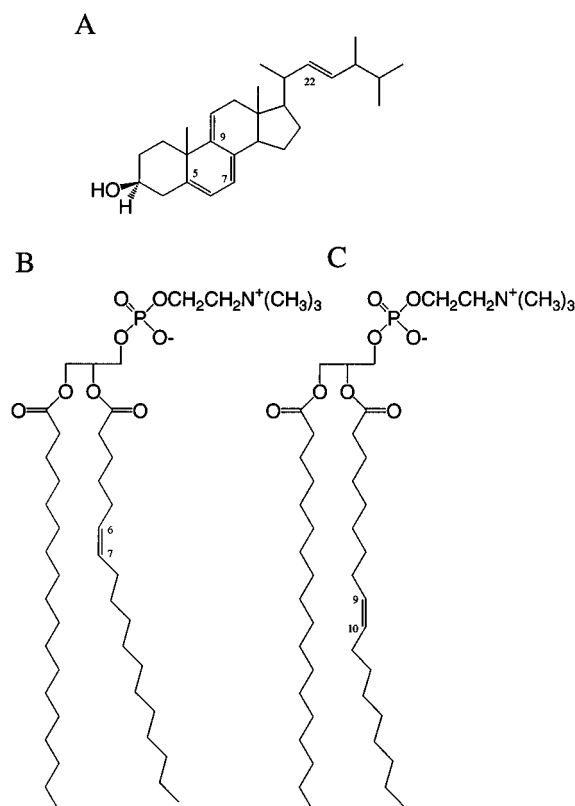


Figure 1. Structures of (A) DHE, (B) C(18:0):C(18:1Δ⁶)PC, and (C) C(18:0):C(18:1Δ⁹)PC.

these PCs varies. The DHE contents in the membranes were varied by ~0.2 mol % in two concentration regions, 18.7–21.3 and 23.9–26.0 mol % DHE. In these two regions, 20.0 and 25.0 mol % are the critical sterol mole fractions predicted for maximal superlattice formation.^{5,7,8,11,14,15} The DHE intensity dips appear at the critical sterol mole fractions in the PC bilayers when the *cis* double bond is located between C9 and the terminal carbon in the *sn*-2 acyl chain. However, no distinct DHE intensity dips are observed in these two concentration regions as well as in the region 18.4–27.5 mol % DHE when the *cis* double bond is located at C6–C7 or C7–C8. These results show additional examples and the limitations of sterol superlattice formation, and shed light on the driving force behind this newly discovered membrane phenomenon.

Materials and Methods

Materials. DHE obtained from Sigma (St. Louis, MO) was re-crystallized from ethanol prior to use. C(18:0):C(18:1Δ⁹)PC and the C(18:0):C(18:1Δ⁶)PC used in Figure 6 were purchased from Avanti Polar Lipids (Alabaster, AL). C(18:0):C(18:1Δ⁶)PC, C(18:0):C(18:1Δ⁷)PC, C(18:0):C(18:1Δ¹¹)PC and C(18:0):C(18:1Δ¹³)PC were a generous gift from Professor Ching-hsien Huang at the University of Virginia. The concentration of DHE was determined using an extinction coefficient at 326 nm equal to 10,600 M⁻¹cm⁻¹ (in dioxane). The phospholipid concentration was determined by the method of Bartlett.¹⁶ The errors of fractional composition resulting from lipid concentration determinations were estimated to be ~0.2 mol %.

Preparation of Liposomes. Multilamellar vesicles (MLVs) were prepared as previously described.^{5,7} In brief, appropriate amounts of DHE and phospholipids were first mixed in chloroform. The mixture was then dried under nitrogen in microtubes (Perfector Scientific, Atascadero, CA) and placed

under high vacuum overnight. The dried mixtures were suspended in 100 mM Tris at pH 7.3. The dispersion was vortexed for 2 min at 42–43 °C, which are well above the main phase transition temperatures of the phospholipids examined. The samples were cooled to 4 °C for 30 min and then incubated at 42–43 °C for 30 min. This cooling/heating cycle was repeated two more times. Finally, the samples were sealed under nitrogen and stored in the dark at room temperature for at least 6 days before fluorescence measurements.

Fluorescence Measurements. Fluorescence intensity measurements were made with an SLM 8000C fluorometer (SLM Instruments, Urbana, IL). Samples were excited at 325 nm with a 1-nm band path. Under this condition, photobleaching was not noticeable during the experiment. The emission was observed at 378 nm through a monochromator with an 8-nm band path. Samples were measured while stirring. The concentration of phospholipids used for fluorescence measurements was ~15 μM. Blank readings from vesicles without DHE were subtracted from the sample readings.

Results

At 37 °C. Figure 2 shows the fractional concentration dependence of DHE fluorescence intensity in C(18:0):C(18:1Δ⁶)PC, C(18:0):C(18:1Δ⁷)PC, C(18:0):C(18:1Δ⁹)PC, C(18:0):C(18:1Δ¹¹)PC, and C(18:0):C(18:1Δ¹³)PC MLVs containing 23.9–26.0 mol % DHE. In this concentration region, 25.0 mol % DHE is the theoretically predicted critical sterol mole fraction for maximal superlattice formation.^{5,11} The y-axis indicates the normalized fluorescence intensities measured at 37 °C, subtracted for blank readings and divided by the amount of DHE in the cuvettes. The normalization means that, in each experimental set, the highest fluorescence intensity is set to unity. At 37 °C, all of the vesicles examined are in the liquid-crystalline state because the main phase transition temperatures of C(18:0):C(18:1Δ⁶)PC, C(18:0):C(18:1Δ⁷)PC, C(18:0):C(18:1Δ⁹)PC, C(18:0):C(18:1Δ¹¹)PC, and C(18:0):C(18:1Δ¹³)PC are 24.8, 16.7, 5.6, 3.8, and 15.9 °C, respectively.^{17,18} In DHE/C(18:0):C(18:1Δ⁹)PC and DHE/C(18:0):C(18:1Δ¹¹)PC bilayers, the fluorescence intensity of DHE decreases when the DHE mole fraction is increased from 23.9 to 25.0 mol % (Figure 2). This is followed by an increase in DHE fluorescence intensity up to ~26.0 mol % DHE. This biphasic change in fluorescence intensity creates an intensity dip at 25.0 mol %, as in the case of DHE in DMPC and sphingomyelin bilayers.^{5–7} This dip concentration is in excellent agreement with the theoretically predicted critical sterol mole fraction, 25.0 mol %. A smaller intensity dip was observed at 24.8 mol % DHE in DHE/C(18:0):C(18:1Δ¹³)PC mixtures (Figure 2). Within the experimental errors (~0.2 mol %), this DHE intensity dip position also agrees with the theoretical value. Noticeably, however, in DHE/C(18:0):C(18:1Δ⁶)PC and DHE/C(18:0):C(18:1Δ⁷)PC bilayers, no distinct intensity dip was observed in the same concentration range examined (23.9–26.0 mol % DHE) (Figure 2).

Similar results were observed in the concentration range 18.7–21.3 mol % DHE in C(18:0):C(18:1Δ⁶)PC, C(18:0):C(18:1Δ⁷)PC, C(18:0):C(18:1Δ⁹)PC, C(18:0):C(18:1Δ¹¹)PC, and C(18:0):C(18:1Δ¹³)PC MLVs at 37 °C (Figure 3). In this concentration region, 20.0 mol % is the only theoretically predicted critical sterol mole fraction. A DHE intensity dip was observed at or very close to 20.0 mol % DHE in C(18:0):C(18:1Δ⁹)PC, C(18:0):C(18:1Δ¹¹)PC, and C(18:0):C(18:1Δ¹³)PC bilayers (Figure 3); however, no intensity dip was detected near this critical mole fraction in C(18:0):C(18:1Δ⁶)PC and C(18:0):C(18:1Δ⁷)PC bilayers (Figure 3).

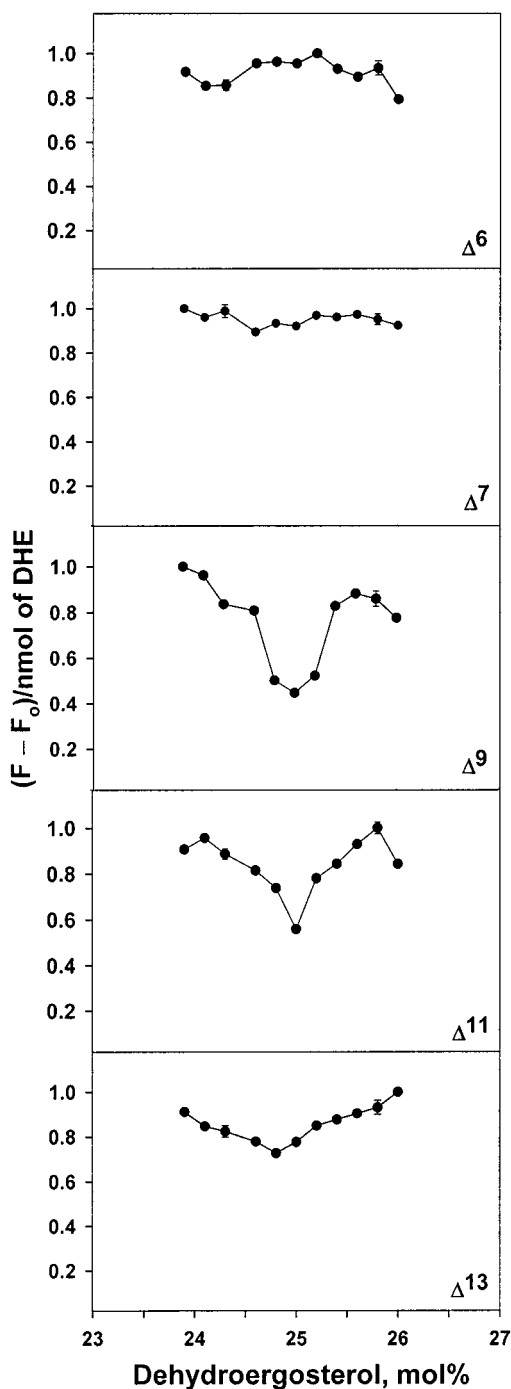


Figure 2. Concentration dependence of DHE fluorescence intensity in C(18:0):C(18:1 Δ^6)PC, C(18:0):C(18:1 Δ^7)PC, C(18:0):C(18:1 Δ^9)PC, C(18:0):C(18:1 Δ^{11})PC, and C(18:0):C(18:1 Δ^{13})PC MLVs in the concentration range 23.9–26.0 mol % at 37 °C. All of the vesicle samples were subject to the same thermal history and the fluorescence measurements were performed on the same day. Typical error bars are shown which represent the standard deviations of fluorescence intensity resulting from three different samples. The y-axis shows the value of the fluorescence intensity measured at 378 nm (F , arbitrary unit) minus the blank reading from vesicles without DHE (F_0), divided by the amount of DHE in the cuvette. The error bars, sample treatment, and y-axis values in Figures 3–7 bear the same meaning.

The lack of distinct DHE intensity dip in DHE/C(18:0):C(18:1 Δ^6)PC bilayers is more clearly seen in Figure 4, where the sterol concentration dependence of the DHE fluorescence intensity in DHE/C(18:0):C(18:1 Δ^6)PC bilayers (dark circles) was examined from 18.4 to 27.5 mol %. In this extended region (covering 9 mole percents), the variation of the DHE fluores-

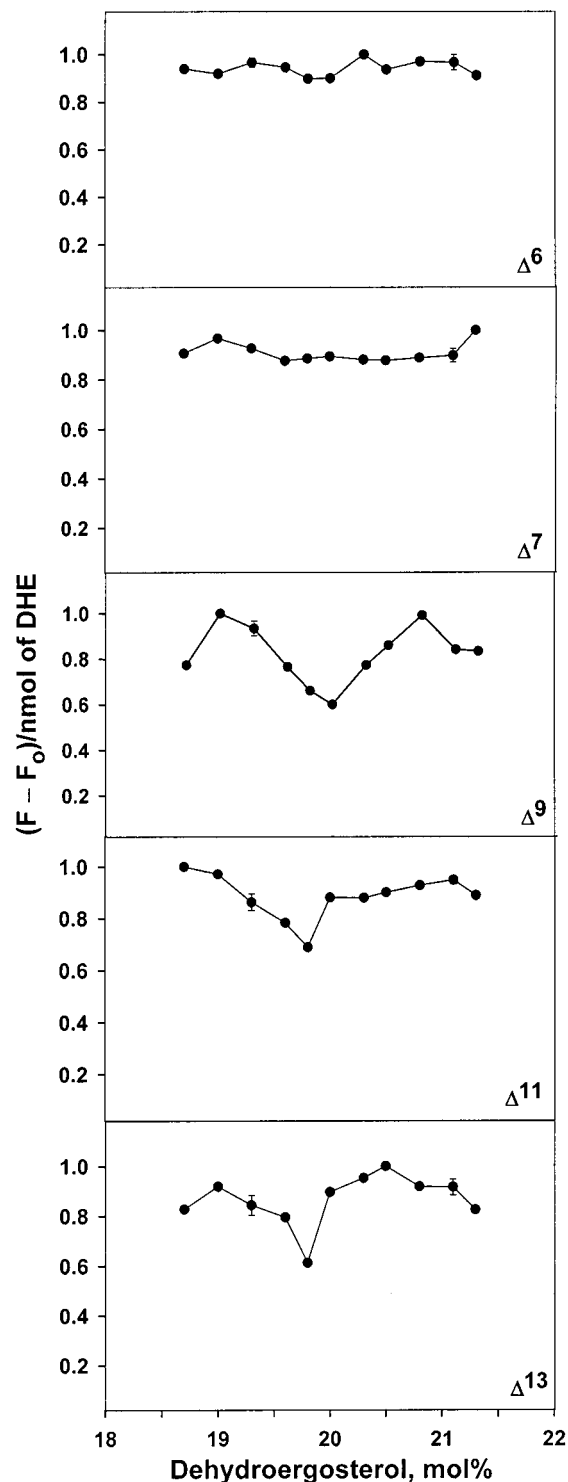


Figure 3. Concentration dependence of DHE fluorescence intensity in C(18:0):C(18:1 Δ^6)PC, C(18:0):C(18:1 Δ^7)PC, C(18:0):C(18:1 Δ^9)PC, C(18:0):C(18:1 Δ^{11})PC, and C(18:0):C(18:1 Δ^{13})PC MLVs in the concentration range 18.7–21.3 mol % DHE at 37 °C.

cence intensity with sterol concentration in C(18:0):C(18:1 Δ^6)PC bilayers appears to be random; and, the amplitude of the intensity variation ($\sim 20\%$ or 0.2) (Figure 4, dark circles) reflects the background noise. The sterol concentration dependence of the DHE fluorescence intensity in C(18:0):C(18:1 Δ^9)PC bilayers is also presented in Figure 4 (open triangles), where distinct DHE intensity dips are seen at 20 mol % (depth = 0.4) and 25 mol % (depth = 0.6), whose depths are much greater than the background noise (0.2 or ± 0.1 around the mean value,

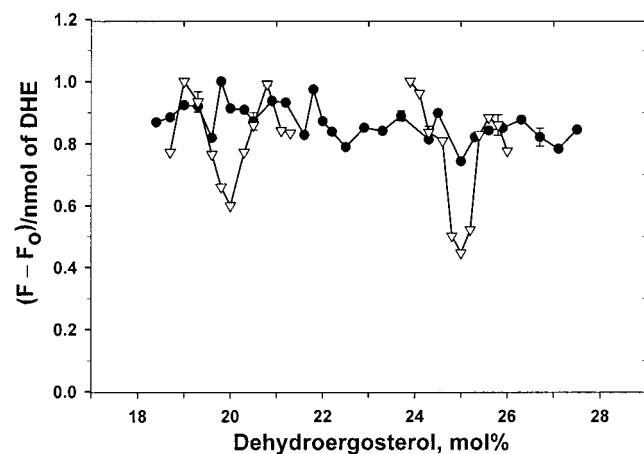


Figure 4. Concentration dependence of DHE fluorescence intensity in C(18:0):C(18:1 Δ^6)PC (dark circles) and C(18:0):C(18:1 Δ^9)PC (open triangles) MLVs in the concentration range 18.4–27.5 mol % DHE at 37 °C.

in agreement with that previously reported¹⁹). The data point at 18.7 mol % in the C(18:0):C(18:1 Δ^9)PC bilayers (Figures 2 and 3) cannot be considered as an intensity dip because a dip requires a biphasic change in intensity on either side of a critical mole fraction. The drop in intensity from 19.0 to 18.7 mol % in the C(18:0):C(18:1 Δ^9)PC bilayers (Figures 2 and 3) is $\sim 20\%$, which probably reflects the background noise. Thus, it can be concluded from Figures 2–4 that all dips that exist appear at critical mole fractions.

To quantitatively emphasize the point that the measured dip at 20 mol % DHE (Figure 4) is twice as large as the noise level, the probability that the dip measured at 20 mol % (Figure 4) is the result of random fluctuation has been calculated and found to be rather small. Assume a Gaussian distribution for the amplitude of the fluctuation and $SD = 0.1$ as standard deviation from the mean value. The dip at 20 mol % DHE contains 2 data points each $2 \times SD$ away from the mean value, and 2 other data points each $4 \times SD$ away from the mean value. The probability of measuring a fluctuation like this is $(0.023)(0.023) \cdot (0.000032)(0.000032) = 5.4 \times 10^{-13}$.

At a Reduced-Temperature 0.076. To ensure that the inability to observe the DHE fluorescence intensity dips in DHE/C(18:0):C(18:1 Δ^6)PC and DHE/C(18:0):C(18:1 Δ^7)PC bilayers at 37 °C (Figures 2–4) is not due to the differences in the phase transition temperatures of the matrix lipids, the experiments were repeated at the same reduced temperature. The fractional concentration dependence of DHE fluorescence intensity in C(18:0):C(18:1 Δ^6)PC, C(18:0):C(18:1 Δ^7)PC, C(18:0):C(18:1 Δ^9)PC, C(18:0):C(18:1 Δ^{11})PC, and C(18:0):C(18:1 Δ^{13})PC MLVs was measured at 47.4, 38.7, 26.8, 25.0, and 37.9 °C, respectively (Figures 5 and 6). At these temperatures, all of the PCs examined are at the same reduced temperature, 0.076. Here, the reduced temperature is defined as $(T - T_m)/(273.2 + T_m)$, where T and T_m stand for the temperatures (in Celsius) for fluorescence measurements and for the main phase transition temperatures of the pure PC bilayers, respectively. Ideally, we should use the T_m 's of the PC bilayers containing the amounts of DHE used in the fluorescence measurements for the calculation of the reduced temperature. However, such T_m values are hard to determine accurately because at high sterol contents (e.g., $> \sim 20$ –25 mol %) the endothermic peak due to the main phase transition of sterol/monounsaturated PC bilayers determined by differential scanning calorimetry is usually very broad and shallow.²⁰ Hence, we consider only the T_m 's of pure C(18:0):C(18:1 Δ^n)PC bilayers and assume that the fractional completion

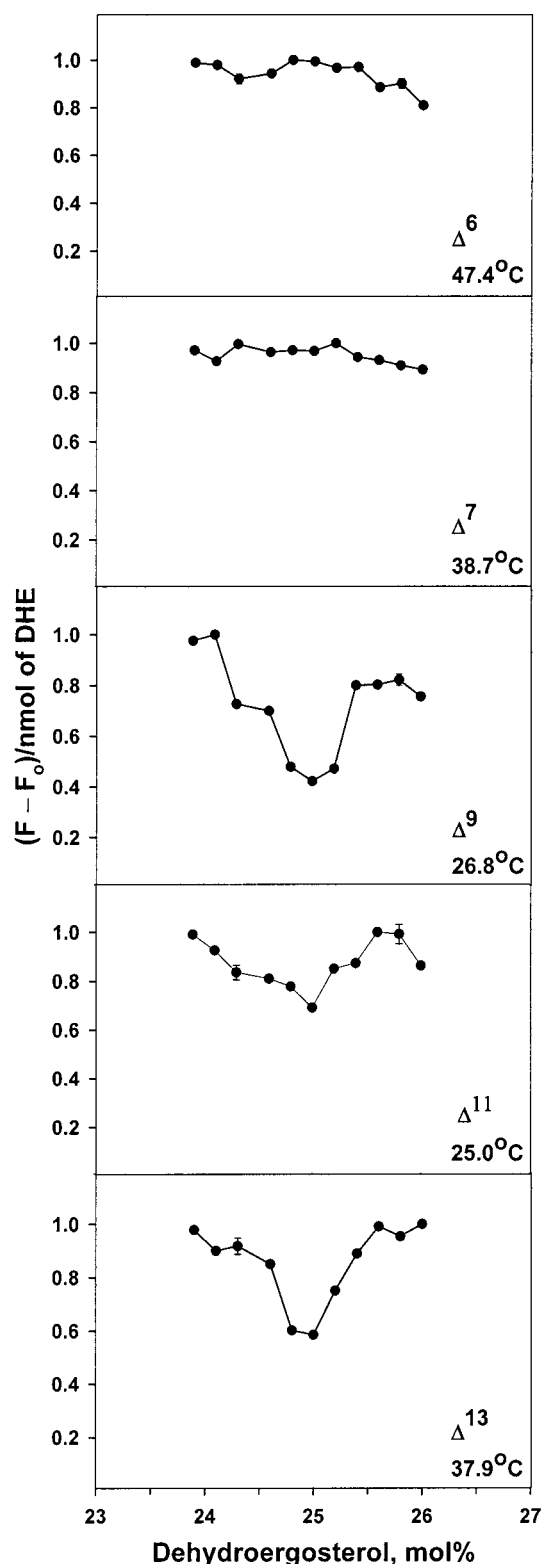


Figure 5. Concentration dependence of DHE fluorescence intensity in C(18:0):C(18:1 Δ^6)PC, C(18:0):C(18:1 Δ^7)PC, C(18:0):C(18:1 Δ^9)PC, C(18:0):C(18:1 Δ^{11})PC, and C(18:0):C(18:1 Δ^{13})PC MLVs in the concentration range 23.9–26.0 mol % at the same reduced temperature 0.076. In each part, the experimental temperature is indicated.

of the gel-to-fluid transition is about the same for the examined PCs at a given reduced temperature.

As shown in Figures 5 and 6, at the same reduced temperature 0.076, a distinct DHE intensity dip is clearly observable at ~ 20.0 and at ~ 25.0 mol % DHE in C(18:0):C(18:1 Δ^9)PC, C(18:0):C(18:1 Δ^{11})PC, and C(18:0):C(18:1 Δ^{13})PC, but not in C(18:0):

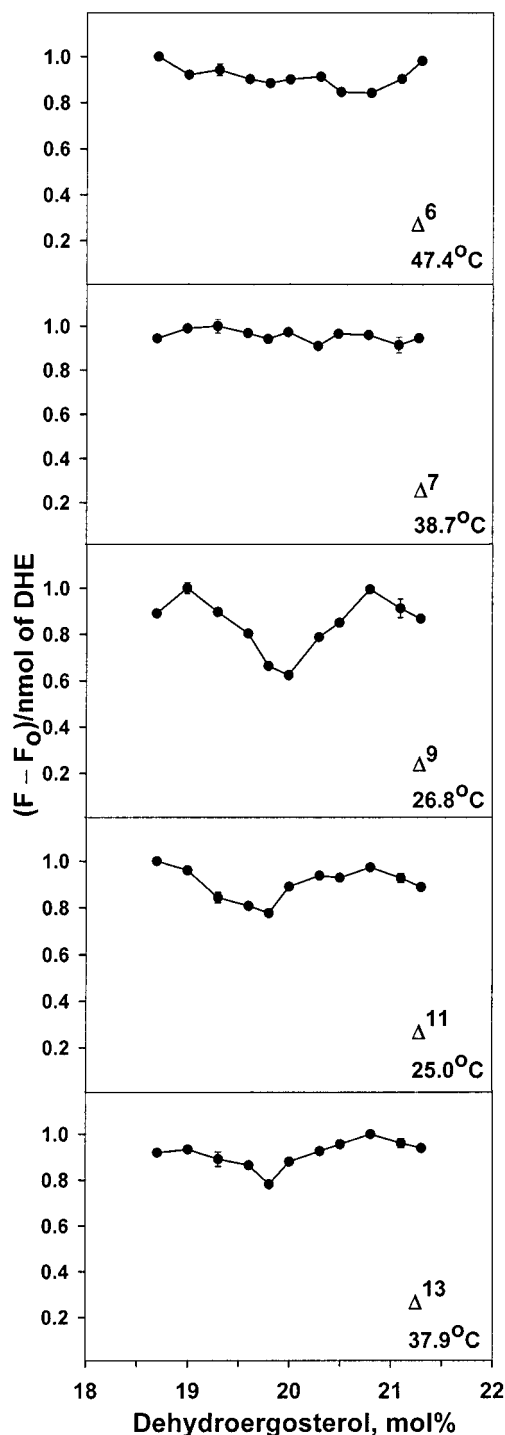


Figure 6. Concentration dependence of DHE fluorescence intensity in C(18:0):C(18:1 Δ^6)PC, C(18:0):C(18:1 Δ^7)PC, C(18:0):C(18:1 Δ^9)PC, C(18:0):C(18:1 Δ^{11})PC, and C(18:0):C(18:1 Δ^{13})PC MLVs in the concentration range 18.7–21.3 mol % DHE at the same reduced temperature 0.076. In each part, the experimental temperature is indicated.

C(18:1 Δ^6)PC and C(18:0):C(18:1 Δ^7)PC bilayers. These results are similar to those obtained at 37 °C (Figures 2 and 3), thus indicating that the inability to observe the DHE dips in DHE/C(18:0):C(18:1 Δ^6)PC and DHE/C(18:0):C(18:1 Δ^7)PC bilayers at 37 °C is not due to the differences in lipid phase state engendered by the different phase transition temperatures of the PC bilayers.

Temperature Effect. The inability to observe the DHE dips in DHE/C(18:0):C(18:1 Δ^6)PC bilayers is not due to the high-temperature induced randomization of lipid lateral organization

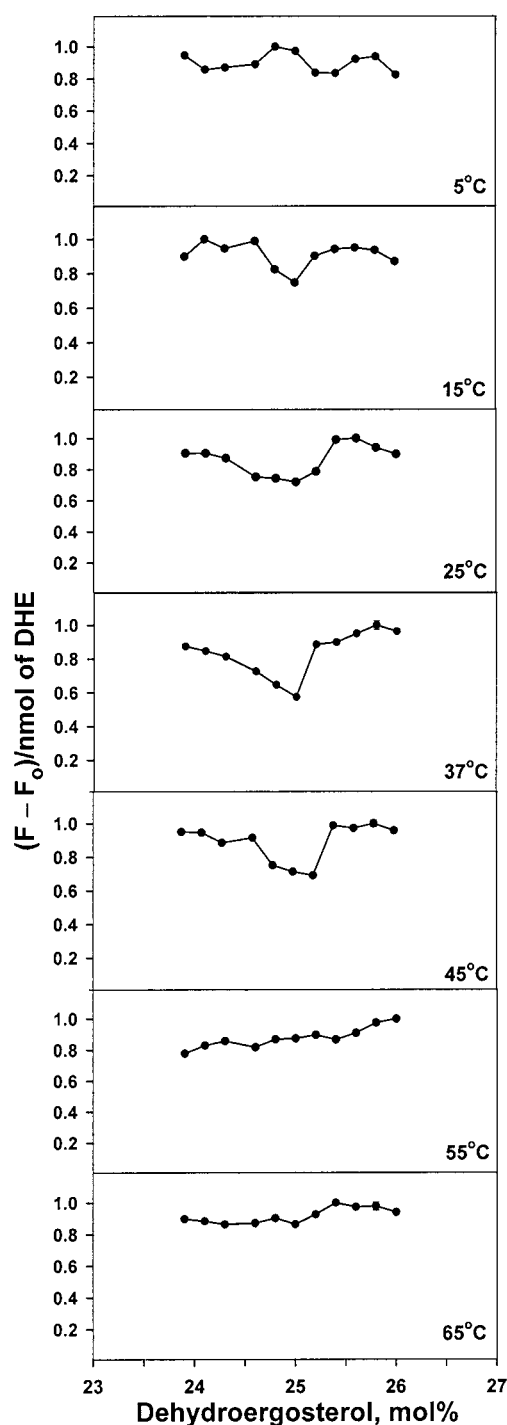


Figure 7. Effect of temperature on the DHE intensity dip near the critical mole fraction 25 mol % DHE in C(18:0):C(18:1 Δ^9)PC MLVs. To compare the DHE dips at different temperatures, all the samples were kept virtually at the same thermal history before fluorescence measurements, using the experimental approaches described in Figure 2 of ref 21. Note that the DHE intensity dips are reproducible as judged by the dip positions.⁷ The shape of the dip (Figure 7 vs the middle part of Figure 2) is less certain because the dip represents a concentration-induced phase transition, at which enhanced data fluctuations are expected.^{8,15,38}

either because this would occur at temperatures higher than 55 °C²¹ (also Figure 7), not at 37 °C (Figures 2 and 3) or 47 °C (Figures 5 and 6). Two additional observations from the data shown in Figure 7 are worth noting. First, the DHE dip at ~25 mol % in DHE/C(18:0):C(18:1 Δ^9)PC bilayers is abolished at ≥ 55 °C (Figure 7). This supports the idea that the DHE dip

results from a phenomenon of self-ordering⁵ and agrees with the temperature data obtained from pyrene-PC/PC bilayers,²¹ another membrane system showing signs of lipid superlattice formation.^{22,23} Second, when the temperature is decreased to 5 °C, which is below the main phase transition temperature of pure C(18:0):C(18:1 Δ^9)PC (T_m = 5.6 °C), the DHE dip is attenuated or abolished, showing only an intensity variation close to the background noise (0.2) (Figure 7). This result indicates that the DHE dips prefer to occur in the liquid-crystalline state. This suggests that sterol superlattices are biologically relevant as most biomembrane lipids are in the fluid state at physiological conditions. Similar conclusions were obtained from lipid superlattices formed by pyrene-containing acyl chains.²¹

In summary, our data (Figures 2–6) clearly indicate that, in fluid bilayers, the DHE intensity dips (inferentially, the evidence of sterol superlattice formation) are observable when the cis double bond is located between C9 and the terminal carbon in the *sn*-2 acyl chain of the phosphatidylcholine molecules. The most prominent dip appears when the cis double bond is located between C9 and C10. However, when the cis double bond is located between C9 and the carboxyl carbon, no distinct DHE dips are detected, thus, showing no evidence for superlattice formation.

Discussion

DHE fluorescence intensity dips have previously been explained via the sterol regular distribution model.^{5,7} According to this model, sterols tend to be maximally separated in the plane of the phospholipid bilayer membrane, thus regularly distributed into hexagonal⁵ or centered rectangular⁸ superlattices. At any given sterol mole fraction, regular (superlattice) distributions always coexist with irregular (nonsuperlattice) distributions, but the ratio of regular to irregular distributions varies with sterol content, reaching a local maximum at the critical sterol mole fractions C_r .^{5,11,15} In the regular regions, lipid packing is tighter because of the stringent lateral arrangements.²¹ The tighter packing leads to either a vertical displacement of sterol toward the aqueous phase or a phospholipid headgroup orientation more perpendicular to the membrane surface or both. As a result, sterol molecules in the regular regions are more exposed to the aqueous phase than those in the irregular regions,⁵ as revealed by the fluorescence quenching data.⁶ Since the regular region is maximal at C_r and the DHE fluorescence intensity decreases with increasing dielectric constant of the medium,²⁴ the fluorescence intensity of DHE drops at C_r .

Based on the idea that the DHE intensity dips originate from sterol superlattice formation, the observation of DHE intensity dips in C(18:0):C(18:1 Δ^9)PC, C(18:0):C(18:1 Δ^{11})PC, and C(18:0):C(18:1 Δ^{13})PC bilayers (Figures 2–6) can be taken to indicate that sterol superlattice occurs when the cis double bond is located between C9 and the terminal carbon in the *sn*-2 acyl chain of the matrix phospholipid. In this case, the depth of the dip reflects the extent of superlattice formation. The absence of distinct DHE dips in C(18:0):C(18:1 Δ^6)PC and C(18:0):C(18:1 Δ^7)PC bilayers, on the other hand, suggests that sterol superlattice is either missing or attenuated when the cis double bond is located between C9 and the carboxyl carbon.

An alternative explanation for the absence of DHE dips in C(18:0):C(18:1 Δ^6)PC and C(18:0):C(18:1 Δ^7)PC bilayers is that sterol superlattices are retained when the cis double bond is located between C9 and the carboxyl carbon, but the changes in the extent of sterol superlattice with sterol mole fraction do not lead to changes in DHE fluorescence intensity. This is possible if the cis double bond in C(18:0):C(18:1 Δ^6)PC and

C(18:0):C(18:1 Δ^7)PC alters the vertical position of DHE such that DHE is more exposed to the aqueous phase. In this case, the DHE fluorescence intensity should become lower as the position of the cis double bond moves toward the glycerol backbone; furthermore, the intensity should become much less sensitive to the changes in the extent of superlattice (the sterol mole fraction). Our data support the latter, but not the former. Figures 2–6 showed little variation in DHE fluorescence intensity with DHE mole fraction in C(18:0):C(18:1 Δ^6)PC and C(18:0):C(18:1 Δ^7)PC bilayers; however, Wang²⁵ showed that at a given temperature (e.g., 37 °C) and a noncritical DHE mole fraction, the DHE fluorescence intensity changed little with the position of cis double bond in C(18:0):C(18:1 Δ^n)PC bilayers (n = 6, 7, 9, 11, and 13), which argues against the alternative explanation.

The differential effect of cis double bond position on DHE dips implies that the van der Waals contacts between the steroid ring and the phospholipid acyl chains may play a critical role in sterol superlattice formation, as explained below. The cis double bond in the C(18:1 Δ^n) acyl chain causes a 120° bent, which would reduce the van der Waals interactions with the neighboring lipids. However, in the liquid-crystalline state, a single gauche configuration may occur at the β -position on either side of the cis double bond. If this β -coupled gauche conformation is followed by a α -carbon rotation about the C=C–C single bond by 30°, then a $\Delta_{n,n+1}tg$ kink will be formed.^{26,27} Here t represents the trans conformation, g the gauche conformation and Δ the position of the cis double bond. As a result, the fatty acyl chain is divided into two linear and parallel segments linked by the $\Delta_{n,n+1}tg$ kink.^{26,27} Due to the lateral displacement of the two linear segments, an upper linear hydrophobic pocket is generated between the carboxyl carbon and the cis double bond.^{26,27} In the cases of C(18:0):C(18:1 Δ^9), C(18:0):C(18:1 Δ^{11}), and C(18:0):C(18:1 Δ^{13})PC bilayers, the upper linear hydrophobic pocket created by the kink has the necessary geometry and dimension (≥ 10 Å) to fit the packing requirements of the two angular methyl groups on the β -surface of the steroid nucleus (~ 9 – 10 Å in length and at the bilayer depth between the carboxyl carbon and C9 of the neighboring acyl chain),^{28,29} permitting favorable van der Waals attractive interactions between the sterol and the fatty acyl chain. In contrast, in C(18:0):C(18:1 Δ^6)PC and C(18:0):C(18:1 Δ^7)PC bilayers, the upper hydrophobic pocket produced by the Δtg kink would be too small to accommodate the steroid ring for appropriate van der Waals contacts. When the van der Waals contacts become inadequate, the DHE dips disappear and sterol superlattices do not form or are attenuated (Figures 2–6).

The idea that direct van der Waals contacts between the steroid ring and the upper linear hydrophobic pocket of the *sn*-2 monoenoic acyl chain are an important determinant of DHE dips or sterol superlattice formation is consistent with previous findings. First, in a previous study of DHE/cholesterol/DMPC, DHE/ergosterol/DMPC, and DHE/cholesterol/DPPC three-component mixtures, the DHE intensity dips and anisotropy peaks were detected whenever the total sterol mole fraction was at or near the critical sterol mole fractions.⁷ In other words, DHE dips appeared regardless of the mixing ratio of DHE to ergosterol (nonfluorescent) or cholesterol (nonfluorescent). Those results supported the notion that sterols are regularly distributed because of the presence of a bulky and rigid tetracyclic steroid ring.⁵ The present study agrees with this notion, but it adds that sterol superlattice formation may also be related to the van der Waals contacts between the steroid ring and its neighboring acyl chain.

Second, our present data are compatible with the previous idea that the cross sectional difference between the steroid ring and the neighboring phospholipid acyl chain plays a key role in lipid superlattice formation. The difference in cross sectional area between the bulky guest lipid molecule (sterol or pyrene-labeled phosphatidylcholine) and the matrix phospholipid acyl chain has previously been thought of as the physical origin for the formation of lipid superlattice. The theory was that the cross sectional difference caused an elastic deformation in the matrix lipid lattice. To minimize the deformation, bulky guest molecules were maximally separated into superlattices in the plane of the membrane as the result of a long-range repulsion.^{5,22,23,30,31} Our present data suggests that, in the mixtures of DHE and C(18:0):C(18:1 Δ^9)PC, C(18:0):C(18:1 Δ^{11})PC, or C(18:0):C(18:1 Δ^{13})PC, the cross-sectional areas of the C2–C9 segments in the *sn*-1 and *sn*-2 acyl chains are virtually identical. Thus, there is a distinct difference in the cross sectional area between the steroid ring and the upper linear regions of the acyl chains. In these mixtures, a DHE intensity dip was observable at or near C_r . In contrast, in the mixtures of DHE and C(18:0):C(18:1 Δ^6)PC or C(18:0):C(18:1 Δ^7)PC, the steroid ring does not fit into the upper linear hydrophobic pocket caused by the Δt_g kink. As a result, the cross sectional area of the upper linear segment in the *sn*-2 acyl chain is greater than that in the *sn*-1 acyl chain. In this case, there is no distinct difference in the cross sectional area between the steroid ring and the upper linear segments of phospholipid acyl chains; in those mixtures, DHE dips were not observed (Figures 2–6).

Third, the assertion that van der Waals attractive interactions between the steroid ring and its neighboring phospholipid acyl chains play a critical role in sterol superlattice formation is consistent with previous computer simulation results. The Monte Carlo simulations of the E/M dips in DMPC/pyrene-labeled phosphatidylcholine mixtures based on long-range and short-range repulsive interactions between bulky lipids were only partially successful as one E/M dip was simulated but the other dips were not.¹⁵ This indicates that repulsion alone is not enough to bring about superlattice formation. More recently, using multibody interactions, Huang and Feigensohn³² were able to simulate superlattice-like structures in cholesterol-containing lipid membranes, which suggests that the direct contacts between sterols and phospholipid acyl chains are an important factor for superlattice formation, a notion consistent with our present finding.

Finally, attractive interactions between sterol and phospholipid are a prerequisite for the formation of “condensed complexes” between cholesterol (or dihydrocholesterol) and phospholipids as reported in recent monolayer studies.^{33,34} This model is compatible with the sterol superlattice model.³³ However, only one stoichiometry of the condensed complexes was reported in a given monolayer system, in contrast to many DHE dips observed at C_r in vesicle bilayer studies.^{5,7,11,12}

We have previously suggested that sterol superlattice occurs not only in saturated phospholipid bilayers (e.g., DMPC), but also in *sn*-1 saturated and *sn*-2 unsaturated phospholipid bilayers with a single cis double bond located between C9 and C10 (e.g., POPC and POPC/POPE).¹¹ The present study extends that sterol superlattice can also occur in other monounsaturated lipid membranes, so long as the cis double bond in the *sn*-2 acyl chain is not located between C2 and C9. This limitation, however, should not be taken to argue against the presence of sterol superlattice in biological membranes because monounsaturated phospholipids with a cis double bond located between the carboxyl carbon and C9 are in small amounts in

mammalian cell membranes.^{35,36} It is conceivable that when small amounts of these phospholipids are mixed with those containing a cis double bond between C9 and the terminal carbon, sterol superlattice structures are retained. Polyunsaturated fatty acyl chains with cis double bonds between C2 and C9 are abundant in cell membranes, especially in the membranes of the nervous system, retina, and spermatozoa. However, recent model membrane studies showed that phospholipids containing highly polyunsaturated fatty acyl chains (e.g., docosahexaenoic acid) are laterally segregated from cholesterol and other lipids.³⁷ This implies that, even in nerve, sperm, and retinal membranes, sterol molecules may still be regularly distributed in the lipid membrane areas separated from highly polyunsaturated lipid domains. Thus, sterol superlattice formation is a viable idea for biological membrane despite the limitation found in the present study.

Acknowledgment. We thank Professor Ching-hsien Huang for the gifts of monounsaturated lipids and for discussion and encouragement. This investigation was supported by a grant from American Heart Association (9950320N) and a grant from Pfizer. Dr. Sugar is also grateful for the support from Mrs. Lawrence Garner.

Nomenclature

DHE, dehydroergosterol, or $\Delta^{5,7,9,(11),22}$ -ergostatetraene-3 β -ol

DMPC, dimyristoyl-L- α -phosphatidylcholine

DPPC, dipalmitoyl-L- α -phosphatidylcholine

MLV, multilamellar vesicles

PC, phosphatidylcholines

POPC, 1-palmitoyl-2-oleoyl-L- α -phosphatidylcholine

POPE, 1-palmitoyl-2-oleoyl-L- α -phosphatidylethanolamine

References and Notes

- (1) Rogers, J.; Lee, A. G.; Wilton, D. D. *Biochim. Biophys. Acta* **1979**, *552*, 23–37.
- (2) Smutzer, G.; Yeagle, P. L. *Biochim. Biophys. Acta* **1985**, *814*, 274–280.
- (3) Bar, L. K.; Chong, P. L.-G.; Barenholz, Y.; Thompson, T. E. *Biochim. Biophys. Acta* **1989**, *983*, 109–112.
- (4) Schroeder, F.; Jefferson, J. R.; Kier, A. B.; Knittel, J.; Scallen, T.; Wood, W. G.; Hapala, I. *Proc. Soc. Exp. Biol. Med.* **1991**, *196*, 235–252.
- (5) Chong, P. L.-G. *Proc. Natl. Acad. Sci. U.S.A.* **1994**, *91*, 10069–10073.
- (6) Chong, P. L.-G.; Liu, F.; Wang, M. M.; Truong, K.; Sugar, I. P.; Brown, R. E. *J. Fluoresc.* **1996**, *6*, 221–230.
- (7) Liu, F.; Sugar, I. P.; Chong, P. L.-G. *Biophys. J.* **1997**, *72*, 2243–2254.
- (8) Virtanen, J. A.; Ruonala, M.; Vauhkonen, M.; Somerharju, P. *Biochemistry* **1995**, *34*, 11568–11581.
- (9) Parasassi, T.; Giusti, A. M.; Raimondi, M.; Gratton, E. *Biophys. J.* **1995**, *68*, 1895–1902.
- (10) Chong, P. L.-G. **1996**, in *High-Pressure Effects in Molecular Biophysics and Enzymology*; Markley, J. L., Northrop, D. B., Royer, C. A., Eds.; Oxford University Press: New York; pp 298–313.
- (11) Wang, M. M.; Sugar, I. P.; Chong, P. L.-G. *Biochemistry* **1998**, *37*, 11797–11805.
- (12) Liu, F.; Chong, P. L.-G. *Biochemistry* **1999**, *38*, 3867–3873.
- (13) Chong, P. L.-G.; Wang, M. M.; Currie, D. S.; Nyugen, M.; Sugar, I. P. *Biophys. J.* **2000**, *78*, 414A.
- (14) Chong, P. L.-G.; Sugar, I. P. *Chem. Phys. Lipids* **2002**, In press.
- (15) Sugar, I. P.; Tang, D.; Chong, P. L.-G. *J. Phys. Chem.* **1994**, *98*, 7201–7210.
- (16) Bartlett, G. R. *J. Biol. Chem.* **1959**, *234*, 466–468.
- (17) Wang, Z.; Lin, H.; Li, S.; Huang, C. *J. Biol. Chem.* **1995**, *270*, 2014–2023.
- (18) Huang, C.; Li, S. *Biochim. Biophys. Acta* **1999**, *1422*, 273–307.
- (19) Parasassi, T.; Gratton, E. *Biophys. J.* **1996**, *70*, 1560–1562.
- (20) Davis, P. J.; Keough, K. M. W. *Biochemistry* **1983**, *22*, 6334–6340.

- (21) Chong, P. L.-G.; Tang, D.; Sugar, I. P. *Biophys. J.* **1994**, *66*, 2029–2038.
- (22) Tang, D.; P. L.-G. Chong. *Biophys. J.* **1992**, *63*, 903–910.
- (23) Somerharju, P. J.; Virtanen, J. A.; Eklund, K. K.; Vainio, P.; Kinnunen, P. K. J. *Biochemistry* **1985**, *24*, 2773–2781.
- (24) Schroeder, F.; Barenholz, Y.; Gratton, E.; Thompson, T. E. *Biochemistry* **1987**, *26*, 2441–2448.
- (25) Wang, M. M. **1999**. Ph.D. Thesis, Temple University School of Medicine, Philadelphia, PA.
- (26) Huang, C. *Lipids* **1977**, *12*, 348–356.
- (27) Huang, C. *Chem. Phys. Lipids* **1977**, *19*, 150–158.
- (28) Ghosh, D.; Williams, M. A.; Tinoco, J. *Biochim. Biophys. Acta* **1973**, *291*, 351–362.
- (29) Worcester, D. L.; N. P. Franks. *J. Mol. Biol.* **1976**, *100*, 359–378.
- (30) Virtanen, J. A.; Somerharju, P.; Kinnunen, P. K. J. *J. Mol. Electron.* **1988**, *4*, 233–236.
- (31) Somerharju, P. J.; Virtanen, J. A.; Cheng, K. H. *Biochim. Biophys. Acta* **1999**, *1440*, 32–48.
- (32) Huang, J.; Feigenson, G. W. *Biophys. J.* **1999**, *76*, 2142–2157.
- (33) Radhakrishnan, A.; McConnell, H. M. *Biophys. J.* **1999**, *77*, 1507–1517.
- (34) Keller, S.; McConnell, H. M. *Phys. Rev. Lett.* **1999**, *82*, 1602–1605.
- (35) Hanahan, D. J. In *A Guide to Phospholipid Chemistry*; Oxford University Press: New York, 1997; pp 7,8.
- (36) Myher, J. J.; Kuksis, A. *Can. J. Biochem.* **1982**, *60*, 638–650.
- (37) Mitchell, D. C.; Litman, B. J. *Biophys. J.* **1998**, *75*, 896–908.
- (38) Nielsen, L. K.; Bjornholm, T.; Mouritsen, O. G. *Nature* **2000**, *404*, 352.